Modeling of Fluid Dynamics and Heat Transfer through Porous Media for Liquid Rocket Propulsion

Emre Sozer[*] and Wei Shyy[†]
University of Michigan, Ann Arbor, MI, 48109

Porous materials are often used for the injector face plate of liquid rocket engines to aid in cooling by transpiration of fuel. A first-principle-based method for predicting fluid flow and heat transfer through porous media is developed to enhance the existing, empirical based methods. In the present approach, the effect of porous structure on the global fluid flow is accounted for via local volume averaged governing equations. The resulting set of transport equations contains closure terms representing the statistical flow characteristics around the pores. These closure terms are deduced by direct computation of the fluid flow in individual, representative pore samples that are observed in the porous material. Hence, empirical dependence of simulations can be removed without requiring excessive computational cost. In this paper, we improve the formulation previously developed by Sozer et al. along with characterization of the Rigimesh porous material.

Nomenclature

A	=	cross-sectional area
A_{sf}	=	solid-fluid interfacial area
C_E	=	Ergun coefficient
δ_{ij}	=	Kronecker delta
ε	=	porosity
K	=	permeability
k_f	=	fluid phase thermal conductivity
k_s	=	solid phase thermal conductivity
$\dot{m}$	=	mass flow rate
μ	=	dynamic viscosity
n_i	=	surface normal vector
p	=	pressure
ρ	=	fluid density
Re_D	=	Reynolds number based on pore diameter
$Re_{\sqrt{K}}$	=	Reynolds number based on permeability
T_{ij}	=	stress tensor
T	=	temperature
u_D	=	filter velocity
u_i	=	velocity vector
V_f	=	volume of the fluid phase
V	=	total volume

I. Introduction

Porous materials are often used for the injector face plate of liquid rocket engines. Fuel bleeds through the porous plate to aid in cooling of the injector face by transpiration. In P&W's RL10 engine and Space Shuttle Main Engine (SSME), Rigimesh porous material is used. Rigimesh can qualitatively be classified as a dense, non-uniform, fibrous porous media (See Figure 1). In the case of SSME, a 0.25" thick plate with about 9% void space is used. Our

---

[*] Graduate Student, Aerospace Engineering Department
[†] Clarence L. "Kelly" Johnson Collegiate Professor and Chair, Aerospace Engineering Department

ultimate goal in this study is accurate simulation of fluid flow and heat transfer through the Rigimesh material. To achieve this, we need detailed knowledge of the material's internal structure.
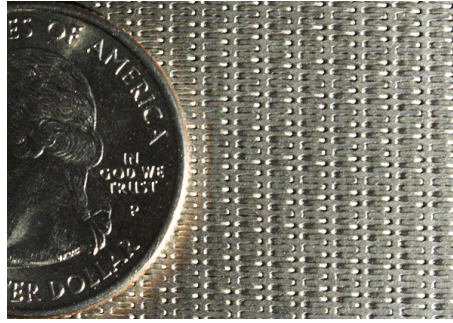

Figure 1. Surface features of the Rigimesh material used in SSME

Fluid flows and associated heat and mass transfer through such porous media are two-phase phenomena where one of the phases is solid and stationary. To simulate such flows, interaction of fluid and solid phases at the scales as small as individual pores of the material needs to be accounted for. Considering typically wide range of length scales and complex geometries involved in porous media, analysis of each individual pore can be very costly or even impossible. Thus the modeling efforts in this area dating back to Darcy's[1] experimental study in 1856 have mostly aimed at empirically correlating the pore level flow effects to the bulk fluid motion. Darcy related the pressure gradient to the average fluid velocity. A commonly adopted form of correlation has been suggested by Ergun[3]. He extended capability of Darcy's relation by adding a quadratic velocity term in order to handle inertial flow regimes. Ergun relation involves two parameters; permeability, K, and Ergun coefficient, C_E, which are determined empirically.

A more fundamental formulation can be developed by averaging the governing equations over local volume elements that contain both fluid and solid phases. Although this will reduce the complexity of the problem, the information lost by filtering the fine scale flow structures will cause an unclosed set of governing equations. Conventionally, the resulting closure terms are heuristically linked to the relations proposed by Darcy and Ergun which requires empirical determination of the parameters K and C_E. To develop non-empirical predictive capabilities for porous media problems, we follow a first principle-based, multi-scale strategy to handle the closure problem. Most porous media can be thought of as a matrix of repeating pore patterns. Instead of directly simulating the fluid flow through the porous material, we model sample pore patterns and calculate the closure terms beforehand for varying flow speeds. Thus, we can avoid the excessive computational cost of direct simulation yet we can produce accurate numerical predictions completely free of empiricism.

In this paper, we first summarize the issues related to the characterization of the Rigimesh material. Then, we briefly review the theoretical background followed by detailed derivations of local volume averaged governing equations. We then explain the conventional and multi-scale closure methodologies. In our multi-scale approach, the effect of porous structure on the global fluid flow is accounted for via local volume averaged governing equations. The resulting set of transport equations contains closure terms representing the statistical flow characteristics around the pores. These closure terms can be deduced by direct computation of the fluid flow in individual, representative pore samples. Hence, empirical dependence of simulations can be removed without requiring excessive computational cost. Formulations presented here contain several corrections over our previously published work[14], including local volume averaged forms of momentum and energy equations and multi-scale estimations of the permeability and the Ergun coefficient. The revised model is incorporated into the Loci-Stream[15] which is a parallel, all-speed CFD code based on the Loci framework. Loci[12] is a rule-based programming framework especially designed for CFD to handle correct coordination of program components, simple storage and query of data, automated scheduling of events and automated parallelism. After introducing Loci-Stream in more detail, we examine the revised methodology for a simple porous medium with well defined pore geometry and compare the predictions to the experimental data by Tully et al.[13]

II. **Rigimesh Characterization**

Rigimesh is a porous material with sintered multiple layers of stainless steel woven-wire-meshes. Bonding of fibers at each contact point due to the sintering process provides rigidity and thus allows finer fiber diameters to be

employed. Finer fiber diameters in effect mean more surface area for a given volume or porosity. These properties make Rigimesh an appropriate fit for the applications that demand high cooling efficiency and rigidity. One such area is the injector face plate of liquid propellant rocket engines.

In order to develop high fidelity models for the simulation of flow and heat transfer through the Rigimesh media, precise understanding of the inner topology as well as the inner dimensions is essential.

In order to characterize the Rigimesh structure, a plate sample of $5.8\ mm$ thickness is examined. Although the surface was hinting a woven structure, examining the cross section was needed to identify the orientation of layers. In order to get a clean cross sectional view of the material, a plate sample is fractured by bending. Although the bending process caused elongation and distortion of the fibers, the cross section view obtained (see Figure 2) gave valuable clues about the inner topology.

Figure 2. Rigimesh cross section after bending fracture

A Rigimesh specimen was analyzed using CT scan. Unfortunately, the CT images didn't have enough resolution to offer more information about the material. The surface properties of the Rigimesh were also examined by the contact profilometer measurement technique. A sensitive needle is traversed along the surface of the Rigimesh plate while maintaining contact. Position of the needle tip is recorded every $0.5\ \mu m$ of a $10\ mm$ span. Lin and Hu[16] have conducted the measurements to characterize the Rigimesh. Their results show that the average distance between the peaks are $0.42\ mm$ which is a measure of distance between fiber axes on the surface. The outcome is presented in Figure 3.
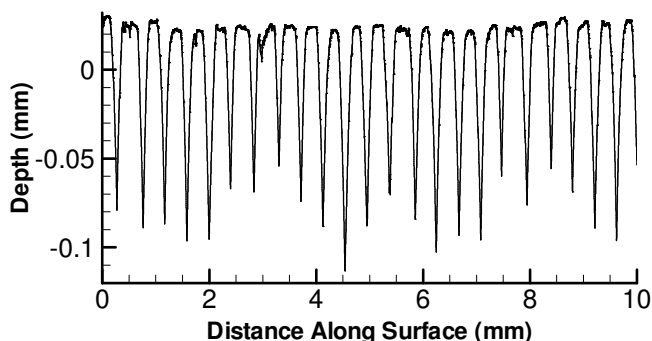

Figure 3. Rigimesh surface characterization by Lin and Hu[16]

The information obtained thus far about the detailed Rigimesh structure is insufficient for developing the pore level computations. More effort is needed.

III.   Multi-Scale Porous Media Model

A. Darcy and Ergun Models

As the first attempt to describe the flow of fluid through porous structures, Darcy[1] experimented with gravity driven flow of water through a porous medium of loosely packed, uniform sized particles. He arrived at the following relation for pressure drop and the flow speed:

$$-\nabla p = \frac{\mu}{K} u_D \tag{1}$$

The permeability, K with the units of $length^2$ is a measure of fluid flow conductivity of the porous media. The filter velocity, u_D, is defined as:

3

$$u_D = \frac{\dot{m}}{\rho A} \tag{2}$$

The linear relationship represented by Darcy's Law has been shown to apply to a wide range of problems as long as a Reynolds number based on permeability, $Re_{\sqrt{K}} = \rho u_D \sqrt{K}/\mu$, is roughly less than unity. At higher Reynolds numbers, inertial effects become comparable to Darcian effects. A correction for this flow regime is suggested by Forchheimer[2] and later by Ergun[3]. Since the form presented here is due to Ergun, we attribute this relation to him.

$$-\partial_i p = \frac{\mu}{K} u_{D_i} + \frac{C_E}{\sqrt{K}} \rho |u_{D_i}| u_{D_i} \tag{3}$$

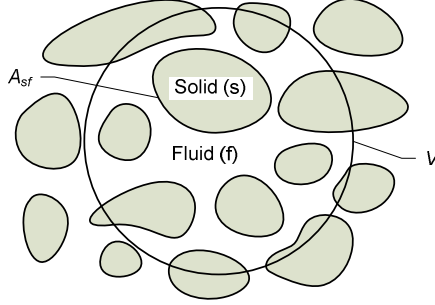## B. Local Volume Averaging

Figure 4. Schematic of a representative elementary volume (REV)

In context of averaging the governing equations, first a sensible scale for an averaging volume needs to be defined. An averaging volume should be sized small enough in order to not filter global flow structures but it should be large enough so as to guarantee containing both fluid and solid phases at all times. In literature, such a volume is called as a representative elementary volume (REV) (see Figure 4). In our multi-scale methodology, we further require an REV to be a repeated pattern over a portion of the porous media.

The porosity, ε, is defined as the volume fraction of fluid phase in a porous media.

$$\varepsilon = \frac{V_f}{V} \tag{4}$$

Note that the porosity might be defined locally or globally depending on the scale that the volume fraction is calculated. In this study, however, we will assume that the porosity is uniform over the porous media.

For an arbitrary property ψ defined for the fluid phase, volume averaging can be carried out as follows[10]:

Intrinsic Averaging:

$$\langle \psi \rangle^f = \frac{1}{V_f} \int_{V_f} \psi dV \tag{5}$$

Superficial Averaging:

$$\langle \psi \rangle = \frac{1}{V} \int_{V_f} \psi dV = \varepsilon \langle \psi \rangle^f \tag{6}$$

C. Averaging of Continuity Equation
The local volume averaged continuity equation can be written as

$$\frac{\partial \langle \rho \rangle}{\partial t} + \langle \partial_i (\rho u_i) \rangle = 0 \tag{7}$$

Note that we want to solve for volume averaged flow quantities. So we need to express the second term in Eq. (7) in terms of $\langle \rho \rangle$ and $\langle u_i \rangle$. The necessary transformation can be achieved via the volume averaging theorem introduced by Slattery[4]:

$$< \partial_i \psi > = \partial_i < \psi > + \frac{1}{V} \int_{A_{sf}} \psi n_i dA \tag{8}$$

4

Here, n_i is the area normal pointing from fluid phase towards solid phase.

Using Eq. (8), Eq. (7) becomes

$$\frac{\partial \langle \rho \rangle}{\partial t} + \partial_i \langle \rho u_i \rangle + \frac{1}{V} \int_{A_{sf}} \rho u_i n_i \mathrm{dA} = 0 \tag{9}$$

Since the fluid will be at rest at the solid-fluid interface due to the no-slip condition, the last term in Eq. (9) vanishes, and we get

$$\frac{\partial \langle \rho \rangle}{\partial t} + \partial_i \langle \rho u_i \rangle = 0 \tag{10}$$

For incompressible flows

$$\partial_i \langle u_i \rangle = 0 \tag{11}$$

Thus, the form of the continuity equation is unchanged by local volume averaging for incompressible flows. In the case of compressible flows, we need to have a special treatment for averaging of the product of the density and the velocity component.

   The derivations hereafter assume incompressible flow with constant properties. We further consider that the porosity is constant throughout the porous media. These aspects can be generalized.

D. Averaging of the Momentum Equation
Averaging the momentum equation with no body forces yields

$$\rho \frac{\partial \langle u_i \rangle}{\partial t} + \rho \langle \partial_j u_i u_j \rangle = \langle \partial_j T_{ij} \rangle \tag{12}$$

Once again, we need to transform the inertial and the stress terms using Eq. (8) so that only the averages of the primitive flow variables are left in the final form instead of averages of their combinations.

1. Inertial Term
Following the approach of Gray[6], we decompose the velocity as

$$u_i = \langle u_i \rangle^f + u_i' \tag{13}$$

where $(\ )'$ represents local deviation from intrinsic averaged values. Applying Eq. (13) to the volume-averaged convective term

$$
\begin{aligned}
\langle \partial_j u_i u_j \rangle &= \langle \partial_j (u_i' + \langle u_i \rangle^f)(u_j' + \langle u_j \rangle^f) \rangle \\
&= \langle \partial_j \langle u_i \rangle^f \langle u_j \rangle^f \rangle + \langle \partial_j u_i' u_j' \rangle + \langle \partial_j \langle u_i \rangle^f u_j' \rangle + \langle \partial_j \langle u_j \rangle^f u_i' \rangle
\end{aligned}
\tag{14}
$$

Using Eq. (8)

$$\langle \partial_j u_i u_j \rangle = \partial_j \langle \langle u_i \rangle^f \langle u_j \rangle^f \rangle + \frac{1}{V} \int_{A_{sf}} \langle u_i \rangle^f \langle u_j \rangle^f n_j \mathrm{dA} + \langle \partial_j u_i' u_j' \rangle + \langle \partial_j \langle u_i \rangle^f u_j' \rangle + \langle \partial_j \langle u_j \rangle^f u_i' \rangle \tag{15}$$

Third and fourth terms can also be treated similarly

$$\langle \partial_j \langle u_i \rangle^f u_j' \rangle = \partial_j \langle \langle u_i \rangle^f u_j' \rangle + \frac{1}{V} \int_{A_{sf}} \langle u_i \rangle^f u_j' n_j \mathrm{dA} \tag{16}$$

Noting that $\langle u_j' \rangle = 0$ and $u_j' = u_j - \langle u_j \rangle^f$

$$\langle \partial_j \langle u_i \rangle^f u_j' \rangle = \frac{1}{V} \int_{A_{sf}} \langle u_i \rangle^f u_j n_j \mathrm{dA} - \frac{1}{V} \int_{A_{sf}} \langle u_i \rangle^f \langle u_j \rangle^f n_j \mathrm{dA} \tag{17}$$

Since the velocity is zero at the solid-fluid interface due to no-slip condition, the first integral term vanishes.

$$\langle \partial_j \langle u_i \rangle^f u_j' \rangle = -\frac{1}{V} \int_{A_{sf}} \langle u_i \rangle^f \langle u_j \rangle^f n_j \mathrm{dA} \tag{18}$$

Thus, Eq. (15) becomes

$$\langle \partial_j u_i u_j \rangle = \partial_j \langle \langle u_i \rangle^f \langle u_j \rangle^f \rangle - \frac{1}{V} \int_{A_{sf}} \langle u_i \rangle^f \langle u_j \rangle^f n_j \mathrm{dA} + \langle \partial_j u_i' u_j' \rangle \tag{19}$$

For the first term on the right hand side of Eq. (19), note that $\langle u_i \rangle^f \langle u_j \rangle^f$ is a constant over the REV and average of the constant quantity is identical to itself. This step is a correction over our previous publication[14]. The correction eliminates an incorrect factor of porosity. Also in this paper, we choose to retain the integral term in Eq. (19) as it is not identically zero unless the pore geometry is symmetric. Note that the same correction is also needed in the convection term of the fluid phase energy equation.

The inertial term now becomes

$$\langle \partial_j u_i u_j \rangle = \partial_j \langle u_i \rangle^f \langle u_j \rangle^f + \langle \partial_j u_i' u_j' \rangle - \frac{\langle u_i \rangle^f \langle u_j \rangle^f}{V} \int_{A_{sf}} n_j \mathrm{dA} \tag{20}$$

Here, the second and the third terms on the right hand side cannot be evaluated with the sole knowledge of averaged flow quantities. These are two of the closure terms we will encounter in the final averaged form of the momentum equation. It is useful to note here that the integral term is identically zero for symmetric REV geometries.

2. Stress Term

For a Newtonian fluid, the stress tensor can be written as

$$T_{ij} = -p\delta_{ij} + \mu(\partial_i u_j + \partial_j u_i) \tag{21}$$

Averaging the stress term of the momentum equation by making use of the volume averaging theorem, i.e. Eq. (8)

$$\langle \partial_j T_{ij} \rangle = -\partial_i \langle p \rangle + \mu \partial_j \langle \partial_i u_j + \partial_j u_i \rangle + \frac{1}{V} \int_{A_{sf}} T_{ij} n_j \mathrm{dA} \tag{22}$$

For the second term on the right hand side, the volume averaging theorem needs to be applied once more.

$$\partial_j \langle \partial_i u_j + \partial_j u_i \rangle = \partial_j \partial_i \langle u_j \rangle + \partial_j^2 \langle u_i \rangle + \partial_j \left(\frac{1}{V} \int_{A_{sf}} (u_i n_i + u_j n_j) \mathrm{dA} \right) \tag{23}$$

For incompressible flows, $\partial_j \langle u_j \rangle = 0$ through the volume averaged continuity equation (Eq. (11)). Also note that the integral term is identically zero due to the fact that the fluid velocity is zero at the solid-fluid interface. Thus the stress term becomes

$$\langle \partial_j T_{ij} \rangle = -\partial_i \langle p \rangle + \mu \partial_j^2 \langle u_i \rangle + \frac{1}{V} \int_{A_{sf}} T_{ij} n_j \mathrm{dA} \tag{24}$$

Using Eqs. (12), (20) and (24), the averaged momentum equation becomes

$$\rho \frac{\partial \langle u_i \rangle}{\partial t} + \frac{\rho}{\varepsilon^2} \partial_j \langle u_i \rangle \langle u_j \rangle$$
$$= -\partial_i \langle p \rangle + \mu \partial_j^2 \langle u_i \rangle - \rho \langle \partial_j u_i' u_j' \rangle + \frac{1}{V} \int_{A_{sf}} T_{ij} n_j \mathrm{dA} + \frac{\rho \langle u_i \rangle^f \langle u_j \rangle^f}{V} \int_{A_{sf}} n_j \mathrm{dA} \tag{25}$$

All the terms of Eq. (25) except the last three on the right hand side are expressed in terms of averaged velocity components, i.e. the knowledge of the bulk fluid motion will suffice in evaluating them. However, the remaining three terms require a closure methodology.

E. Closure of Momentum Equation

Direct computation of Eq. (25) necessitates complete knowledge of fluid flow throughout the porous media. Most porous media applications require a high number of pores for effective cooling or filtering. Therefore, the direct computation approach is rarely feasible. Answer to this problem has conventionally been to find empirical parameters for each porous material that would connect the closure terms to the bulk fluid motion. At this point, we take an alternate route and take advantage of the fact that most porous media consist of a matrix of repeating pore patterns. So, instead of computing the flow field in each pore, we can try to get away with modeling a single one of each repeating pore patterns observed in a given porous media. The closure terms for each pore model can then be computed for a range of flow speeds, allowing us to construct the closure terms accurately as functions of position and flow speed:

$$\rho \frac{\partial \langle u_i \rangle}{\partial t} + \frac{\rho}{\varepsilon^2} \partial_j \langle u_i \rangle \langle u_j \rangle = -\partial_i \langle p \rangle + \mu \partial_j^2 \langle u_i \rangle + S(x_j, u_j) \tag{26}$$

Where $S(x_j, u_j)$ is the closure functional established via the multi-scale method. Note that the closure functional acts as a source term in the local volume averaged momentum equation. Thus, existing Navier-Stokes solvers can be used to compute this kind of problems with very little modification for the porous zones. Computational cost associated with this multi-scale approach strongly depends on the level of uniformity and complexity of the pores. For a uniform porous media, only one pore model is needed.

It is useful to compare and relate the conventional and multi-scale methods of closure. In the conventional method, the closure terms in Eq. (25) are linked to the Ergun relation (Eq. (3)) as

$$\rho \frac{\partial \langle u_i \rangle}{\partial t} + \frac{\rho}{\varepsilon^2} \partial_j \langle u_i \rangle \langle u_j \rangle = -\partial_i \langle p \rangle + \mu \partial_j^2 \langle u_i \rangle - \frac{\mu}{K} \langle u_i \rangle - \frac{C_E}{\sqrt{K}} \rho |\langle u_i \rangle| \langle u_i \rangle \tag{27}$$

While Eq. (3) only relates the bulk pressure drop to the total mass flow rate, the solution of Eq. (27) provides local volume averaged flow field information throughout the porous media. Eq. (27) is very similar in form to the Navier-Stokes equations. This enables us to easily handle both conjugate open flow (without porous media) and porous flow problems and permits application of no-slip conditions at the solid walls bounding the solid matrix. By this treatment, the problem is reduced to the determination of two parameters, namely, permeability, K and Ergun coefficient, C_E. These parameters are either estimated through existing empirical correlations or found via experiments for specific types of porous media. Note that there is no fundamental reason for Eq. (27) to be correct. However, in most tightly packed porous media, momentum loss is largely due to the pore scale flow structures. In these cases, porous source terms are dominant over the other terms in the averaged momentum equation. Thus, generally, Eq. (27) is expected to closely follow Eq. (3). Note also that Eq. (27) does not provide a fully computational framework for porous media problems as opposed to the multi-scale method. Another drawback of the conventional method is that it assumes the permeability and the Ergun coefficient to be independent of the flow speed for a given porous material. We will show later that this is in fact not the case.

Comparing Eqs. (25) and (27), we can find the permeability and the Ergun coefficient for a given flow speed with the multi-scale method instead of experimentation

$$K = -\mu \langle u_i \rangle \left[\frac{1}{V} \int_{A_{sf}} T_{ij} n_j \mathrm{dA} \right]^{-1} \tag{28}$$

$$C_E = \frac{\sqrt{K}}{|\langle u_i \rangle| \langle u_i \rangle} \left[\langle \partial_j u_i' u_j' \rangle - \frac{\langle u_i \rangle^f \langle u_j \rangle^f}{V} \int_{A_{sf}} n_j \mathrm{dA} \right] \tag{29}$$

F. Averaging of the Energy Equation
Consider the fluid phase energy equation with constant specific heat and no heat sources

$$(\rho c_p)_f \left(\frac{\partial T_f}{\partial t} + \partial_i u_i T_f \right) = k_f \partial_j^2 T_f \tag{30}$$

Applying local volume averaging

$$(\rho c_p)_f \left(\frac{\partial \langle T_f \rangle}{\partial t} + \langle \partial_i u_i T_f \rangle \right) = k_f \langle \partial_j \partial_j T_f \rangle \tag{31}$$

Using Eq. (8), the diffusive term can be expanded as

$$k_f \langle \partial_j \partial_j T_f \rangle = k_f \partial_j \langle \partial_j T_f \rangle + \frac{k_f}{V} \int_{A_{sf}} n_j \partial_j T_f \mathrm{dA} = k_f \partial_j^2 \langle T_f \rangle + \frac{k_f}{V} \partial_j \int_{A_{sf}} n_j T_f \mathrm{dA} + \frac{k_f}{V} \int_{A_{sf}} n_j \partial_j T_f \mathrm{dA} \tag{32}$$

Defining a local temperature deviation as

$$T_f = \langle T_f \rangle^f + T_f' \tag{33}$$

and employing the divergence theorem, the first integral term in Eq. (32) becomes

$$\int_{A_{sf}} n_j T_f \, \mathrm{d}A = \int_{A_{sf}} n_j \langle T_f \rangle^f \, \mathrm{d}A + \int_{A_{sf}} n_j T_f' \, \mathrm{d}A = \int_V \partial_j \langle T_f \rangle^f \, \mathrm{d}V + \int_{A_{sf}} n_j T_f' \, \mathrm{d}A \tag{34}$$

Noting that the variation of an averaged quantity within the averaging volume itself is zero, the first integral vanishes. We then arrive at the averaged diffusion term

$$k_f \langle \partial_j \partial_j T_f \rangle = k_f \partial_j^2 \langle T_f \rangle + \frac{k_f}{V} \partial_j \int_{A_{sf}} n_j T_f' \, \mathrm{d}A + \frac{k_f}{V} \int_{A_{sf}} n_j \partial_j T_f \, \mathrm{d}A \tag{35}$$

Averaging of the convection term yields:

$$\langle \partial_i u_i T_f \rangle = \partial_i \langle u_i T_f \rangle + \frac{1}{V} \int_{A_{sf}} u_i T_f n_i \, \mathrm{d}A \tag{36}$$

The integral term on the right hand side of Eq. (36) vanishes due to no-slip condition at the solid-fluid walls. Using Eq. (33), we decompose the convective term as

$$\langle \partial_i u_i T_f \rangle = \partial_i \langle (\langle u_i \rangle^f + u_i')(\langle T_f \rangle^f + T_f') \rangle = \partial_i \langle \langle u_i \rangle^f \langle T_f \rangle^f + \langle u_i \rangle^f T_f' + u_i' \langle T_f \rangle^f + u_i' T_f' \rangle \tag{37}$$

Knowing that $\langle \psi' \rangle = 0$, the volume-averaged convection term is obtained

$$\langle \partial_i u_i T_f \rangle = \partial_i \langle u_i \rangle^f \langle T_f \rangle^f + \varepsilon \partial_i \langle u_i' T_f' \rangle^f \tag{38}$$

Substituting Eq. (38) and Eq. (35) in Eq. (31), we obtain the volume-averaged energy equation for the fluid phase

$$\varepsilon (\rho c_p)_f \left(\frac{\partial \langle T_f \rangle^f}{\partial t} + \frac{1}{\varepsilon} \partial_i \langle u_i \rangle^f \langle T_f \rangle^f + \partial_i \langle u_i' T_f' \rangle^f \right)$$
$$= \varepsilon k_f \partial_j^2 \langle T_f \rangle^f + \frac{k_f}{V} \partial_j \int_{A_{sf}} n_j T_f' \, \mathrm{d}A + \frac{k_f}{V} \int_{A_{sf}} n_j \partial_j T_f \, \mathrm{d}A \tag{39}$$

Similarly, for the solid phase, the volume-averaged energy equation is

$$(1 - \varepsilon)(\rho c_p)_s \frac{\partial \langle T_s \rangle^s}{\partial t} = (1 - \varepsilon) k_s \partial_j^2 \langle T_s \rangle^s + \frac{k_s}{V} \partial_j \int_{A_{fs}} n_j T_s' \, \mathrm{d}A + \frac{k_s}{V} \int_{A_{fs}} n_j \partial_j T_s \, \mathrm{d}A \tag{40}$$

In many practical problems, the temperature difference between the solid and fluid phases inside an REV is much smaller than the global scale temperature variation. This condition is met if the REV is much smaller compared to global length scale, there is no heat generation or loss inside the REV and temperature distribution does not vary or vary slowly over time. Under these conditions, we can assume "local thermodynamic equilibrium" (LTE) which grants

$$\langle T_f \rangle^f = \langle T_s \rangle^s = \langle T \rangle \tag{41}$$

At the solid-fluid interface, the following boundary conditions apply

$$T_f' \big|_{A_{sf}} = T_s' \big|_{A_{sf}} \tag{42}$$

$$k_f \partial_j T_f \big|_{A_{sf}} = k_s \partial_j T_s \big|_{A_{sf}} \tag{43}$$

Also noting that $\mathbf{n}_{sf} = -\mathbf{n}_{fs}$, and adding Eqs.(39) and (40), we obtain the local volume averaged energy equation

$$\left[\varepsilon (\rho c_p)_f + (1 - \varepsilon)(\rho c_p)_s \right] \frac{\partial \langle T \rangle}{\partial t} + \frac{1}{\varepsilon} (\rho c_p)_f \partial_i \langle u_i \rangle \langle T \rangle$$
$$= \left[\varepsilon k_f + (1 - \varepsilon) k_s \right] \partial_j^2 \langle T \rangle + \frac{k_f - k_s}{V} \partial_j \int_{A_{sf}} n_j T_f' \, \mathrm{d}A - \varepsilon (\rho c_p)_f \partial_i \langle u_i' T_f' \rangle^f \tag{44}$$

Eq. (44) introduces two additional closure terms for non-isothermal problems. These closure terms can be handled the same way as the momentum equation counterparts with the multi-scale method. The last two terms on the right hand side of Eq. (44) can be computed over the chosen sample pore models for a range of temperature values. In the current work, we will focus on an isothermal problem. However, we presented the derivation of the local volume averaged energy equation for completeness and as a step towards our goal of simulating the transpiration cooling of the liquid rocket engine injector face plate.

8

In summary, the present model has improved several aspects in comparison with that developed by Sozer et al.[14], including a more general form derived by retaining the last integral term seen in the volume averaged momentum equation (Eq. (25)), also reflected in the multi-scale Ergun coefficient expression (Eq. (29)) and the corrected porosity factors in volume averaged momentum and energy equations (Eqs. (25) and (44)), again reflected in multi-scale permeability and Ergun coefficient expressions (Eqs. (28) and (29)).

IV.   Numerical Method and Assessment of the Present Porous Media Model

We have shown that the local volume averaged continuity equation is unchanged and momentum equation is very similar in form to the regular Navier-Stokes equations with additional momentum source terms and the convection term modified by a factor of porosity squared, ε^2. Thus a Navier-Stokes solver can easily be modified to account for porous media.

The proposed formulation has been implemented in an existing Navier-Stokes solver called Loci-STREAM[15]. Loci-STREAM is an all-speed, pressure-based, parallel finite volume solver that is capable of handling arbitrary polyhedral unstructured meshes. Porous zones are designated by coordinate ranges and the previously calculated source terms are added to the momentum equation components.

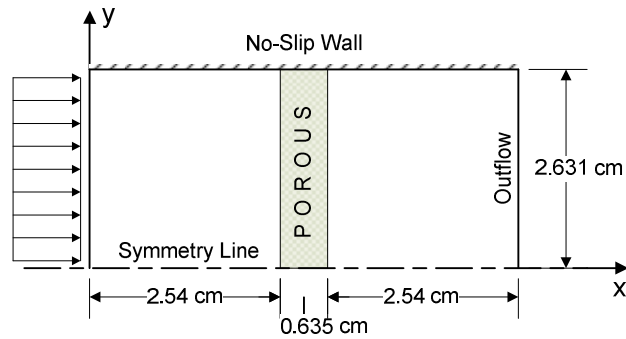### A. Isothermal Flow through a Drilled Orifice Plate

Figure 5. Problem domain

This test case consists of a porous plate placed in a cylindrical channel as shown in Figure 5. The porous material used herein is a metallic plate with an array of uniform and evenly distributed drilled holes. Due to its simple and well defined pore geometry, this case is attractive for testing the multi-scale method developed here. The hole pattern details are shown in Figure 6.
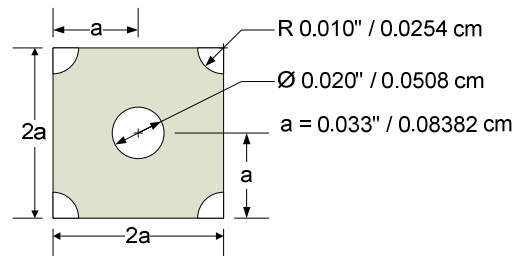

Figure 6. Hole pattern details

This problem was studied before by Tully et al.[13] both numerically and experimentally. The porous plate was inserted in a cylindrical channel test section and pressure drop values were recorded for a range of average flow speeds as summarized in Table 1.

9

Table 1. Summary of experimental conditions.

Fluid properties (Air @ 24.2 °C)			Inlet Filter Velocities (m/s)	
Density (ρ)	1.1875	kg/m^3	U_{D1}	13.1
Dynamic Viscosity (μ)	1.8048E-5	$kg/m.s$	U_{D2}	16.3
Specific Heat (c_P)	1006.2	$J/kg.K$	U_{D3}	18.1
Thermal Conductivity (k)	0.025913	$W/m.K$	U_{D4}	20.1
			U_{D5}	23.3
			U_{D6}	25.8

1. Pore Model

The porous metallic plate has a uniform array of circular through holes distributed along its surface. Therefore, the pore shape is simply a circular tube. In order to account for the momentum loss as the flow adjusts to enter the pores, we extend the pore domain for 3 hole diameters towards upstream direction.

Isothermal fluid flow through the pore is computed for the range of flow speeds listed in Table 1. Eqs. (28) and (29) are evaluated to find the permeability and Ergun coefficient for each flow speed in conjunction with Eq. (27) for the global domain. Results of the pore-scale analysis are listed in Table 2.

Table 2. Pore-scale analysis results

U_D (m/s)	Re_D	K (m^{-2})	C_E
13.1	438	2.29×10^{-10}	1.38×10^{-2}
16.3	545	1.92×10^{-10}	1.26×10^{-2}
18.1	605	1.76×10^{-10}	1.21×10^{-2}
20.1	672	1.61×10^{-10}	1.15×10^{-2}
23.3	779	1.43×10^{-10}	1.08×10^{-2}
25.8	862	1.30×10^{-10}	1.03×10^{-2}

Table 2 clearly shows that in contrast to conventional assumption, permeability and the Ergun coefficient vary significantly with changing flow speeds and are not material properties.

2. Global Domain

With the closure parameters obtained via the pore-scale analysis, flow through the global domain as shown in Figure 5 is computed. In the porous zone, Navier-Stokes equations are replaced with Eq. (27). Pressure drop values across the centerline is plotted in comparison to the experimental results by Tully et al.[13] in Figure 7.
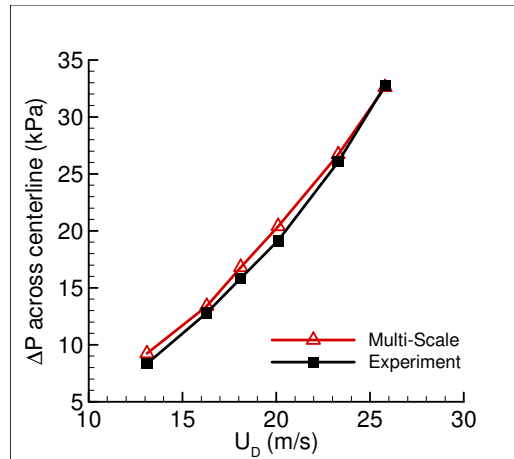

Figure 7. Pressure drop across centerline vs. filter velocity

Figure 7 shows that the experimental data is closely reproduced by the multi-scale method. The error relative to the experimental data ranges between 11% and 1% for the lowest and highest flow speeds respectively.

V.   Summary and Conclusion

We have improved the strategy initially proposed by Sozer et al.[14] for multi-scale numerical simulations of fluid flow through porous media. In the present model, the effect of porous structures on the global fluid flow is accounted for via local volume averaged governing equations, while the closure terms are accounted for via averaging flow characteristics around the pores. Hence, empirical dependence of simulations is removed without requiring excessive computational cost. The performance of the model has been tested for an isothermal flow case. Both the permeability and Ergun coefficient are shown to be flow properties as opposed to the empirical approach which typically results in constant values of these parameters independent of the flow conditions. Hence, the present multi-scale approach is more versatile and can account for the possible changes in flow characteristics.

Although only demonstrated for an isothermal flow case through a simple porous media, the model can easily be extended to more complex flow types and geometries. Our main motivation in this study is to accurately predict the cooling due to fuel flow through the Rigimesh material. The formulation presented is incorporated into Loci-STREAM code which will allow us flexibility in dealing with such complex problems.

In the present model, detailed characterization of the topology and the dimensions of the pore patterns is needed. To date, the Rigimesh characterization efforts have not yet provided such information. More efforts are needed in this aspect.

References

[1] Darcy H., *Les Fontaines Publiques de la ville de Dijon*, Dalmont, Paris, 1856.

[2] Forchheimer P., "Wasserbewegung durch Boden," *Z Ver Deutsch Ing*, 45:1782-1788, 1901.

[3] Ergun S., "Fluid Flow Through Packed Column," *Chem Eng Prog* 48:89-94, 1952.

[4] Slattery J. C., "Single-phase Flow through Porous Media," *AICHE J* 15:866-872, 1969.

[5] Ward J. C., "Turbulent Flow in Porous Media," *J Hyd Div ASCE* 90(HY5):1-12, 1969.

[6] Gray, W.G., "A Derivation of the Equations for Multiphase Transport," Chem. Engng. Sci. 30, 229-233, 1975.

[7] Nozad, I., Carbonell, R. G., Whitaker, S., "Heat Conduction in Multi-Phase Systems I: Theory and Experiments for Two-Phase Systems," *Chem. Engng. Sci.*, 40, 843-855, 1985.

[8] Shyy, W., *Computational Modeling for Fluid Flow and Interfacial Transport, Elsevier Science Publishers*, Amsterdam, 1994.

[9] Kaviany, M., *Principles of Heat Transfer in Porous Media*, Springer-Verlag, New York, 1995

[10] du Plesis P., *Fluid Transport in Porous Media*, Computational Mechanics Publications, Southampton, 1997.

[11] Martin A., Saltiel C., Shyy W., "Frictional Losses and Convection Heat Transfer in Sparse, Periodic Cylinder Arrays in Cross Flow," *Int J Heat Mass Transfer* 41:2383-2397, 1998.

[12] Luke E. and George T., "Loci: A Rule-Based Framework for Parallel Multidisciplinary Simulation Synthesis", *Journal of Functional Programming, Special Issue on Functional Approaches to High-Performance Parallel Programming*, Volume 15, Issue 03, 2005, pp. 477-502, Cambridge University Press, 2005

[13] Tully L. R., Omar, A., Chung, J. N., and Carroll, B. F., "Fluid flow and heat transfer in a liquid rocket fuel injector," *AIAA/ASME/SAE/ASEE Joint Propulsion Conference & Exhibit*, AIAA-2005-4127, 2005.

[14] Sozer, E., Shyy, W. and Thakur S., "Multi-Scale Porous Media Modeling for Liquid Rocket Injector Applications", 42nd *AIAA/ASME/SAE/ASEE Joint Propulsion Conference & Exhibit,* AIAA-2006-5046, 2006

[15] Kamakoti, R., Thakur, S., Wright, J., Shyy, W., "Validation of a New Parallel All-Speed CFD Code in a Rule-Based Framework for Multidisciplinary Applications", *36th AIAA Fluid Dynamics Conference and Exhibit*, AIAA 2006-3063, 2006

[16] Lin, G. and Hu, J., Department Mechanical Engineering, University of Michigan, Private Communication, 2007.